# Effects of thymoquinone against angiotensin II-induced cardiac damage in apolipoprotein E-deficient mice

LEI ZHANG[1], HUJIN ZHANG[2], JING MA[1], YUN WANG[1], ZUOWEI PEI[3,4] and HUI DING[1]

[1]Department of Cardiology, Xi'an No. 3 Hospital, Xi'an, Shaanxi 710018; [2]Department of Neurosurgery, Xi'an Central Hospital, Xi'an, Shaanxi 710000; [3]Department of Cardiology, Beijing Hospital; [4]National Centre of Gerontology, Institute of Geriatric Medicine, Chinese Academy of Medical Sciences, Beijing 100730, P.R. China

Received November 24, 2021; Accepted February 17, 2022

DOI: 10.3892/ijmm.2022.5119

**Abstract.** Herbal medicines have attracted much attention in recent years and are increasingly being used as alternatives to pharmaceutical medicines. Thymoquinone (TQ) is one of the most active ingredients in *Nigella sativa* seeds, which has several beneficial properties, including anti-inflammatory, anti-oxidative stress, anti-hypertensive, anti-apoptotic and free radical-scavenging effects. Angiotensin II (Ang II) is involved in cardiovascular diseases. The present study aimed to investigate the potential protective effects of TQ against Ang II-induced cardiac damage in apolipoprotein E-deficient ($ApoE^{-/-}$) mice. Briefly, 8-week-old male $ApoE^{-/-}$ mice were randomly divided into four groups: Control, TQ, Ang II and Ang II + TQ groups. Osmotic minipumps, filled with either a saline vehicle or an Ang II solution (1,000 ng/kg/min), were implanted in $ApoE^{-/-}$ mice for up to 4 weeks. The serum levels of high-sensitivity C-reactive protein (hs-CRP) and histopathological alterations in heart tissue were assessed. In addition, the mRNA and protein expression levels of molecules associated with fibrosis (collagen I and III), oxidative stress and apoptosis (Nox4 and p53), and inflammation [tumor necrosis factor (TNF)-α, interleukin (IL)-1β and IL-6] were analyzed by reverse transcription-quantitative PCR (RT-qPCR) and western blotting. In the *in vitro* study, H9c2 cells were incubated with different concentrations of Ang II, and the expression levels of pro-inflammatory cytokines were evaluated using RT-qPCR, whereas the protein expression levels of phosphorylated-extracellular signal-regulated kinase (p-ERK) were determined using western blotting. Western blotting was also performed to detect the expression levels of collagen I, collagen III, Nox4 and p53 in H9c2 cells. The results revealed that TQ inhibited the Ang II-induced increases in serum hs-CRP levels. TQ also significantly inhibited the high levels of TNF-α, IL-1β, IL-6, collagen I, collagen III, Nox4 and p53 in Ang II-treated mice. Furthermore, TQ protected against Ang II-induced cardiac damage by inhibiting inflammatory cell infiltration, proinflammatory cytokine expression, fibrosis, oxidative stress and apoptosis by suppressing activation of the p-ERK signaling pathway. In conclusion, TQ could be considered a potential therapeutic agent for Ang II-induced cardiac damage.

## Introduction

Angiotensin II (Ang II) is known to be a major effector peptide of the renin-angiotensin system (RAS), and serves an important role in regulating blood pressure and humoral homeostasis (1). Epidemiological and experimental data have suggested that RAS activation serves an important role in increasing the risk of cardiovascular events (2). Substantial evidence has suggested that Ang II, as a RAS effector peptide, may be involved in the development of cardiovascular diseases, such as atherosclerosis (3). In humans, associative evidence has indicated that cardiovascular events increase alongside increases in renin activity (3). In mice, injections of Ang II have been reported to promote cardiovascular disease, such as atherosclerosis, abdominal aortic aneurysms and cardiac hypertrophy (4-6). Several mechanisms may underlie how Ang II promotes cardiac damage. Firstly, Ang II may indirectly influence cardiovascular disease development by increasing arterial blood pressure (7). Secondly, Ang II has been reported to possess numerous properties directly affecting cardiovascular disease, including pro-inflammatory (8), fibrosis-enhancing (9) and oxidative stress-promoting effects (10).

Thymoquinone (TQ) is the most abundant constituent of the volatile oil of *Nigella sativa* seeds and the majority of the properties of this plant are primarily attributed to TQ (11). The molecular formula of TQ is $C_{10}H_{12}O_2$. TQ has been reported to exhibit anti-inflammatory, anti-oxidative stress, anti-hypertensive, anti-apoptotic and free radical-scavenging

*Correspondence to:* Dr Hui Ding, Department of Cardiology, Xi'an No. 3 Hospital, 10 East Section of Fengcheng Third Road, Xi'an, Shaanxi 710018, P.R. China
E-mail: dhdinghui007@163.com

*Abbreviations:* TQ, thymoquinone; Ang II, angiotensin II; $ApoE^{-/-}$, apolipoprotein E-deficient; hs-CRP, high-sensitivity C-reactive protein; RT-qPCR, reverse transcription-quantitative PCR; IL, interleukin; TNF-α, tumor necrosis factor α; ECM, extracellular matrix; MAPK, mitogen-activated protein kinase

*Key words:* TQ, ApoE, cardiac damage, *Nigella sativa*, Ang II

properties (12-14). There has been a growing interest in the use of TQ as an alternative treatment for several conditions, including cardiovascular diseases. Xiao *et al* (15) reported that TQ effectively improved cardiac function in rats with ischemia/reperfusion injury, inhibited oxidative stress, decreased myocardial enzyme activity and reduced myocardial infarct size. In addition, other studies have revealed that TQ could attenuate cisplatin-induced cardiac damage and morphine-induced cardiac cell apoptosis in rats (16,17). However, the effects of TQ on Ang II-induced cardiac damage remain unclear. H9c2 cells are often used to study the mechanisms associated with cardiac damage; therefore, the present study established an Ang II-induced cardiac damage model to examine the role of TQ and its potential mechanism in H9c2 cells. Furthermore, apolipoprotein E-deficient ($ApoE^{-/-}$) mice are commonly used as a model of Ang II-induced aortic aneurysm (18,19). Since Ang II has an important role in the development of atherosclerosis, the present study conducted a series of experiments using this model and monitored organ damage in $ApoE^{-/-}$ mice. The kidney, arteries and heart were described in other studies; however, the present study focused on cardiac damage.

## Materials and methods

*Animal maintenance*. $ApoE^{-/-}$ male mice (n=30; weight, 24.30±1.04 g) were purchased from Beijing Vital River Laboratory Animal Technology Co., Ltd. All mice were housed in a room at a constant temperature of 23-25˚C and 40-60% humidity under a 12-h light/dark cycle. The mice had free access to water and food. At 8 weeks of age, the mice were equally and randomly divided into four groups as follows: Control group (n=7), TQ group (n=7), Ang II group (n=8) and TQ + Ang II group (n=8). TQ (50 mg/kg/d; cat. no. 490-91-5; MilliporeSigma) was administered to the TQ and TQ + Ang II groups by gavage (20). Osmotic minipumps (Model 2004; ALZET® Osmotic Pumps; Durect Corporation), filled with either saline vehicle or Ang II solution (1,000 ng/kg/min; cat. no. 4474-91-3; MilliporeSigma), were implanted subcutaneously in mice for up to 4 weeks (21). Each group of mice was subjected to their respective treatment for 4 weeks. Blood pressure was measured using photoplethysmography using a computerized tail-cuff system (BP-2000 Blood Pressure Analysis System; Visitech Systems) in conscious animals, as previously described (22). After 4 weeks, the mice were weighed and then sacrificed with a high dose of pentobarbital (100 mg/kg, intraperitoneal administration), and a lack of respiration and heartbeat was used as an indicator of mouse death. Blood samples were obtained from the abdominal cava, collected in serum tubes and stored at -80˚C until further use. In addition, the hearts were weighed and coronal sections of heart tissues were fixed in 10% formalin for 30 min, dehydrated in 75% ethanol overnight and finally embedded in paraffin for histological evaluation at room temperature (24-26˚C). The remaining heart tissues were stored at -80˚C and later used to perform reverse transcription-quantitative PCR (RT-qPCR) or western blot analysis. All experimental procedures in the present study were approved by the ethical committee of Xi'an No. 3 Hospital (Xi'an, China).

*Biochemical analysis*. Serum was obtained from the abdominal aorta of mice and preserved in tubes. The blood samples were immediately centrifuged at 1,006 x g for 10 min at 4˚C after collection and the serum was subsequently stored at -80˚C. Serum high-sensitivity C-reactive protein (hs-CRP) was measured using an ELISA kit (cat. no. SEKM-0059; Beijing Solarbio Science & Technology Co., Ltd.) according to the manufacturer's protocol. Total cholesterol (TC; cat. no. A111-1-1), triglyceride (TG; cat. no. A110-1-1) and low-density lipoprotein cholesterol (LDL-c; cat. no. A113-1-1) levels were examined using commercial reagent kits (Nanjing Jiancheng Bioengineering Institute).

*Cardiac histological analysis*. Cardiac tissues were fixed in 10% formalin for 30 min, dehydrated in 75% ethanol overnight and finally embedded in paraffin for histological evaluation at room temperature (24-26˚C). According to manufacturer's protocol, serial sections (4 $\mu$m) were subjected to staining with a hematoxylin and eosin (H&E) staining kit (cat. no. G1120; Beijing Solarbio Science & Technology Co., Ltd.) and Masson's trichrome stain kit (cat. no. G1340; Beijing Solarbio Science & Technology Co., Ltd.) at room temperature (24-26˚C) and according to the manufacturer's protocol to assess pathological changes. Blue staining indicated collagen accumulation in Masson's trichrome staining. Images of the sections were analyzed using ImageJ software v1.8.0 (National Institutes of Health). The mean cross-sectional area and fibrosis of cardiomyocytes were assessed by computerized planimetry.

*Cell culture and treatment*. Rat cardiac H9c2 cells were purchased from the National Collection of Authenticated Cell Cultures (cat. no. GNR 5, http://www.nccc.com/) and were cultured in Dulbecco's modified Eagle's medium (cat. no. D0819; MilliporeSigma) containing 10% fetal calf serum (cat. no. 10099141; Gibco; Thermo Fisher Scientific, Inc.), 100 U/ml penicillin-streptomycin (cat. no. V900929; MilliporeSigma). H9c2 cells were maintained at 37˚C in a humidified atmosphere containing 5% $CO_2$ and were treated with different doses of Ang II (0, 150 and 300 nmol/l) for 24 h. Cells underwent RNA and protein extraction, and the expression levels of pro-inflammatory cytokines were assessed using RT-qPCR and p-ERK expression levels were detected using western blotting. In addition, cells were pre-incubated with an ERK inhibitor (20 $\mu$mol PD98059; cat. no. HY-12028; MedChemExpress) for 30 min [PD98059 was dissolved in DMSO (0.4 $\mu$l/ml; cat. no. D8371; Beijing Solarbio Science & Technology Co., Ltd.)], followed by treatment with Ang II (300 nmol/l) for 48 h at 37˚C. For TQ treatment, cells were grown to 80% confluence and were then incubated with TQ at the indicated concentration (20 $\mu$mol/l) for 24 h when treated with Ang II at the same time. TQ treatment was used to detect the effects of TQ on p-ERK. For PD + Ang II + TQ group, the cells were pre-incubated with PD and then treatment with Ang II and TQ as previously mentioned. DMSO treatment (final concentration, 0.1%) was used as a sham control for all cell groups. The treated cells were harvested and washed with PBS for the subsequent analyses.

*RNA isolation and RT-qPCR*. The primers were designed by Invitrogen; Thermo Fisher Scientific, Inc. Total RNA was isolated from cardiac tissue and cells using the TransZol Up Plus

Table I. Primer sequences used for reverse transcription-quantitative PCR.

| Gene | Primer sequence |
|---|---|
| Mouse TNF-α | F: 5'-TCTCATGCACCACCATCAAGGACT-3' |
| | R: 5'-ACCACTCTCCCTTTGCAGAACTCA-3' |
| Mouse IL-6 | F: 5'-TACCAGTTGCCTTCTTGGGACTGA-3' |
| | R: 5'-TAAGCCTCCGACTTGTGAAGTGGT-3' |
| Mouse IL-1β | F: 5'-TGCCACCTTTTGACAGTGAT-3' |
| | R: 5'-TGTGCTGCTGCGAGATTTGA-3' |
| Mouse β-actin | F: 5'-CGATGCCCTGAGGGTCTTT-3' |
| | R: 5'-TGGATGCCACAGGATTCCAT-3' |
| Rat TNF-α | F: 5'-CACCACGCTCTTCTGTCTACTG-3' |
| | R: 5'-GCTACGGGCTTGTCACTCG-3' |
| Rat IL-6 | F: 5'-CTTCCATCCAGTTGCCTTCTTG-3' |
| | R: 5'-AATTAAGCCTCCGACTTGTGAAG-3' |
| Rat IL-1β | F: 5'-GTGGCAGCTACCTATGTCTTGC-3' |
| | R: 5'-CCACTTGTTGGCTTATGTTCTGT-3' |
| Rat β-actin | F: 5'-CCTGTGGCATCCATGAAACTAC-3' |
| | R: 5'-CCAGGGCAGTAATCTCCTTCTG-3' |

F, forward; IL, interleukin; R, reverse; TNF-α, tumor necrosis factor-α.

RNA kit (cat. no. ER501-01; Transgen Biotech Co., Ltd.) and cDNA was synthesized using TransScript® One-Step gDNA Removal and cDNA Synthesis SuperMix (cat. no. AT311-02; Transgen Biotech Co., Ltd.) according to the manufacturer's protocols. Gene expression was analyzed quantitatively by qPCR using the TransStart® Top Green qPCR SuperMix kit (cat. no. AQ131-01; Transgen Biotech Co., Ltd.). β-actin cDNA was amplified and quantified in each cDNA preparation to normalize the relative amounts of the target genes. The cDNA amplification was performed as follows: The first cycle was maintained at 95c for 30 sec, followed by 38 cycles consisting of denaturation (95˚C for 10 sec), annealing (60˚C for 20 sec), and extension (72˚C for 15 sec). The IL-1β, TNF-α and IL-6 were then processed using the $2^{-\Delta\Delta Cq}$ method (23), during which a single calibrated sample was compared against the gene expression of every unknown sample. Primer sequences are listed in Table I.

*Immunohistochemistry*. Coronal sections of heart tissues were fixed in 10% formalin for 30 min, dehydrated in 75% ethanol overnight and finally embedded in paraffin for histological evaluation at room temperature (24-26˚C). For immunohistochemical staining, the heart sections were deparaffinized with xylene (two times, 10 min each) and rehydrated in a descending alcohol series (100, 90, 80 and 70% alcohol; 5 min each). Subsequently, the sections were blocked with 3% $H_2O_2$ in methanol for 15 min at room temperature to inactivate endogenous peroxidases, and incubated overnight at 4˚C with the following primary antibodies: Rabbit anti-collagen I antibody (cat. no. 14695-1-AP; 1:200; Wuhan Sanying Biotechnology), rabbit anti-collagen III antibody (cat. no. 22734-1-AP; 1:200; Wuhan Sanying Biotechnology), rabbit anti-Nox4 antibody (cat. no. 14347-1-AP; 1:200; Wuhan Sanying Biotechnology) and rabbit anti-p53 antibody (cat. no. 10442-1-AP; 1:200; Wuhan Sanying Biotechnology). The sections were washed three times in water containing PBS (5 min/wash) and subsequently incubated with a goat anti-rabbit HRP-conjugated secondary antibody (Histofine Simple Stain kit; cat. no. 414321; Nichirei Biosciences, Inc.) for 30 min at room temperature. All sections were examined under an Olympus B 40X upright light microscope (Olympus Corporation).

*Western blot analysis*. Proteins were extracted from cardiac tissues and cells using radioimmunoprecipitation assay buffer (cat. no. P0013B; Beyotime Institute of Biotechnology). Cardiac tissue total protein concentrations were determined using a BCA Protein assay reagent kit (cat. no. DQ111-01; Beijing Transgen Biotech Co., Ltd.). The protein samples (20 $\mu$g per lane) were then separated by sodium dodecyl sulfate-polyacrylamide gel electrophoresis on 10% gels and transferred to polyvinylidene fluoride membranes (cat. no. IPFL00010; MilliporeSigma). The membranes were blocked with 5% skim milk in TBS containing 0.1% Tween-20 at room temperature for 1 h and then incubated with the primary antibodies at 4˚C overnight. Primary rabbit antibodies against phosphorylated (p)-extracellular signal-regulated kinase (ERK) (cat. no. 9102; 1:1,000; Cell Signaling Technology, Inc.), collagen I (cat. no. 14695-1-AP; 1:1,000; Wuhan Sanying Biotechnology), collagen III (cat. no. 22734-1-AP; 1:1,000; Wuhan Sanying Biotechnology), Nox4 (cat. no. 14347-1-AP; 1:1,000; Wuhan Sanying Biotechnology), p53 (cat. no. 10442-1-AP; 1:1,000; Wuhan Sanying Biotechnology), total (t)-ERK (cat. no. 11257-1-AP; 1:1,000; Wuhan Sanying Biotechnology) and β-actin (cat. no. 4970; 1:1,000; Cell Signaling Technology, Inc.) were used. After the membranes were washed, they were incubated with the appropriate anti-rabbit IgG secondary antibody (cat. no. 7074; 1:2,000; Cell Signaling Technology, Inc.) for 1 h at room temperature (24-26˚C). Enhanced chemiluminescence

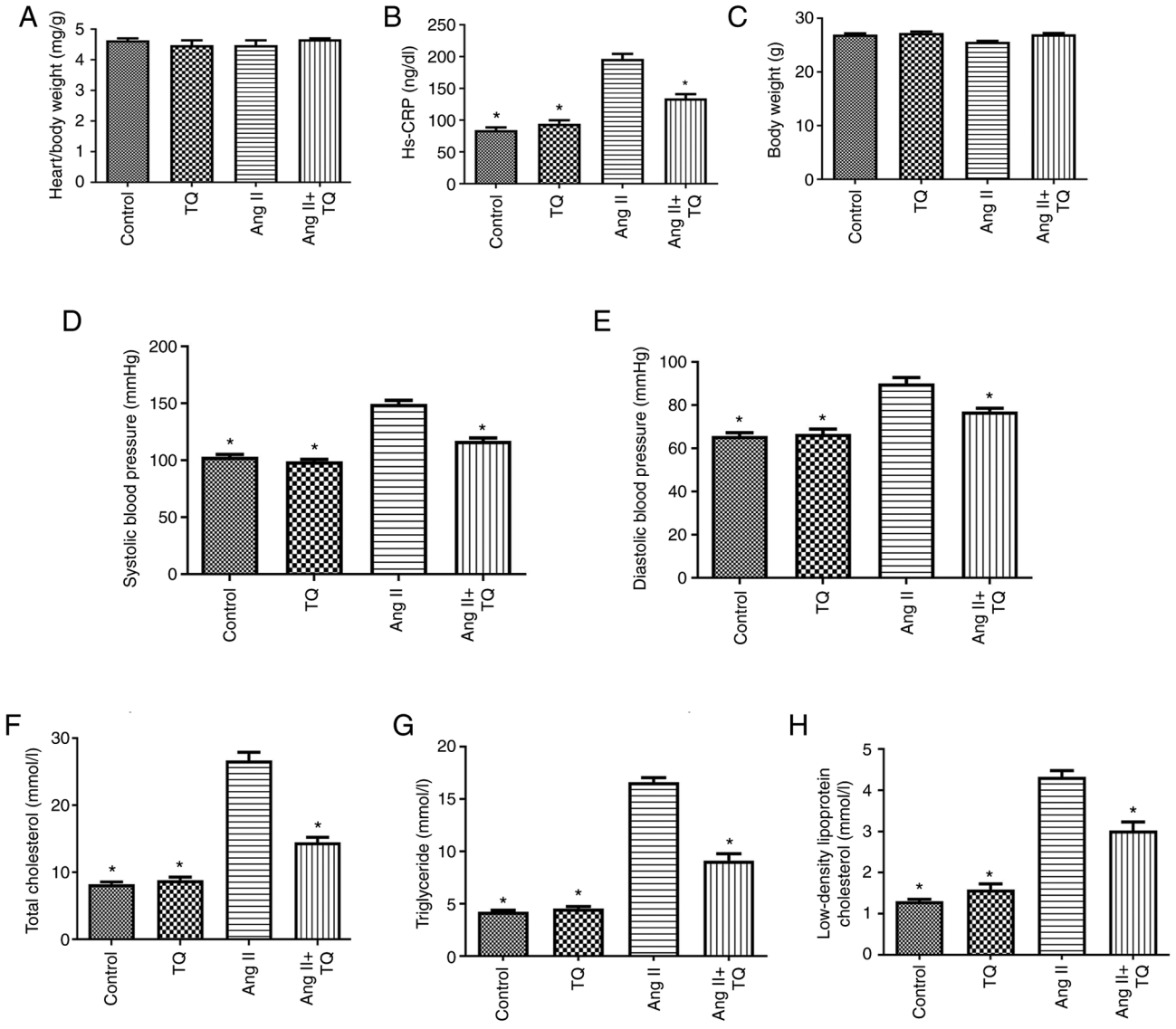


Figure 1. Metabolic data showing the (A) heart/body weight, (B) hs-CRP, (C) body weight, (D) systolic blood pressure, (E) diastolic blood pressure, (F) total cholesterol, (G) triglyceride and (H) low density lipoprotein cholesterol of the mice in the four groups after different treatments. Data are presented as the mean ± SEM; n=6-8/group. *P<0.05 vs. the Ang II group. Hs-CRP, high-sensitivity C-reactive protein; TQ, thymoquinone; Ang II, angiotensin II. TC, TG and LDL-c.

reagent (cat. no. 32106; Thermo Fisher Scientific, Inc.) was used to visualize bands. Signals were imaged using a Bio-Rad imaging system (Bio-Rad Laboratories, Inc.) with a Chemi 410 HR camera (Analytik; Jena AG) and analyzed using Gel-Pro Analyzer version 4.0 (Media Cybernetics, Inc.). The analysis was performed independently three times. The blotted proteins were semi-quantified using ImageJ software version 1.8.0 (National Institutes of Health). β-actin was used as an internal control and protein expression levels were expressed as protein/β-actin ratios, but this was not the case for p-ERK; t-ERK was used as an internal control for p-ERK.

*Statistical analysis*. Data are expressed as the mean ± SEM and were analyzed using SPSS 23.0 statistical software (IBM Corporation). Intergroup statistical significance of multiple groups was determined using one-way ANOVA, followed by Tukey's test. Differences between two groups was determined using one-way ANOVA without a post hoc test. There were three experimental repeats. P<0.05 was considered to indicate a statistically significant difference.

## Results

*Metabolic characterization*. The metabolic characteristics of the mice in the four groups are shown in Fig. 1. No differences in body and heart/body weight were detected among the groups. Notably, a significant increase was observed in the serum levels of hs-CRP, TC, TG and LDL-c in the Ang II group compared with those in the control group, which was significantly decreased upon TQ treatment. Furthermore, an increase in blood pressure was detected in the Ang II group compared with that in the control group. Notably, TQ suppressed this increase in blood pressure in mice in the Ang II + TQ group.

*TQ reduces the histopathological changes in the heart tissues of mice in the Ang II group*. To evaluate histopathological

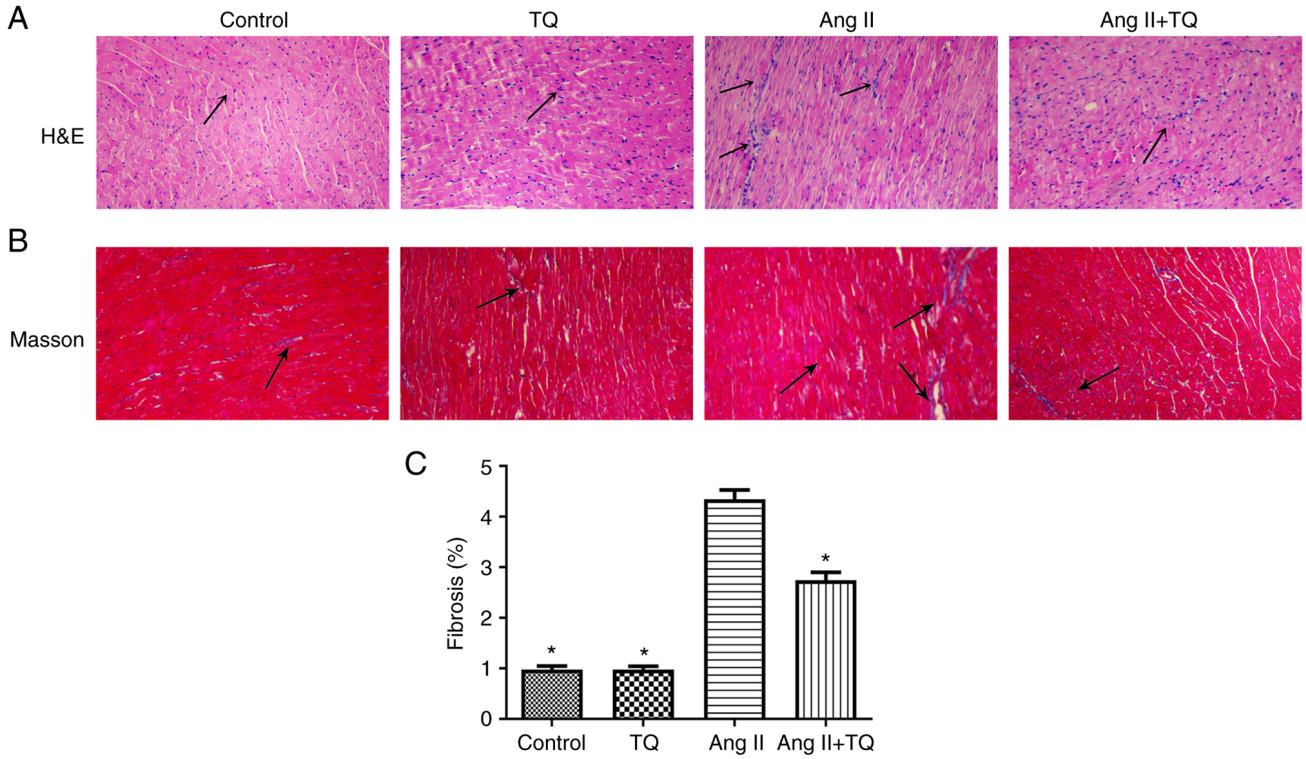


Figure 2. Histology of injuries. (A) H&E and (B) Masson staining of mouse heart tissues from the four groups following different treatments. Arrows indicate tissue damage. Magnification, x40. n=3/group. (C) The bar graph shows semi-quantification of the area of cardiac fibrosis from Masson trichrome-stained sections. Data are presented as the mean ± SEM; n=3/group *P<0.05 vs. the Ang II group. H&E, hematoxylin and eosin; TQ, thymoquinone; Ang II, angiotensin II.

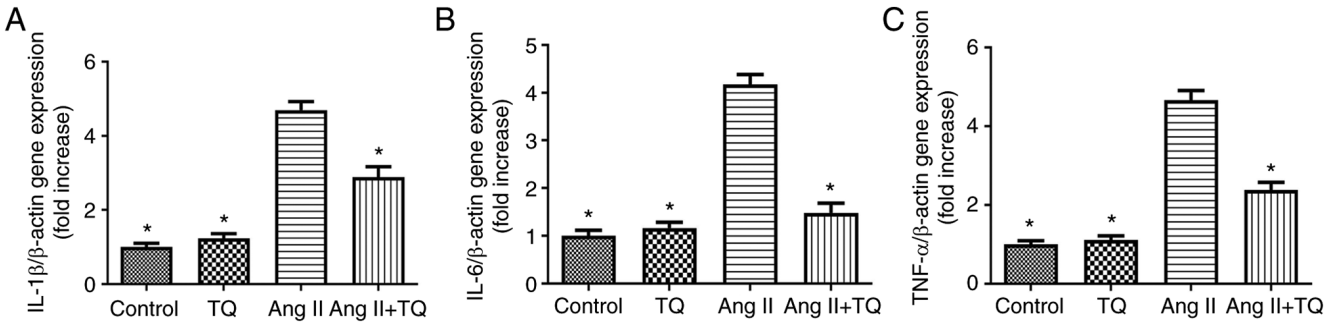


Figure 3. Relative mRNA expression levels of (A) IL-1β, (B) IL-6 and (C) TNF-α in heart tissue from mice in the four groups after different treatments. Data are presented as the mean ± SEM; n=5-7/group. *P<0.05 vs. the Ang II group. IL, interleukin; TNF-α, tumor necrosis factor α; TQ, thymoquinone; Ang II, angiotensin II.

changes in heart tissues, H&E and Masson staining were performed (Fig. 2). Heart tissues from the control group appeared normal; however, histopathological changes, including inflammatory cell infiltration and collagen deposition, were observed in the heart tissues of Ang II-treated mice. Notably, this damage was suppressed in Ang II + TQ mice. The area of cardiac fibrosis from Masson trichrome-stained sections were clearly increased in Ang II group, while TQ treatment suppressed this increased.

*TQ reduces pro-inflammatory cytokine expression in the heart tissues of mice in the Ang II group*. To evaluate the involvement of pro-inflammatory cytokines in mouse heart tissue, the mRNA expression levels of IL-1β, IL-6 and TNF-α were measured using RT-qPCR in the different mouse groups (Fig. 3). The expression levels of these three genes were increased in Ang II-treated mice compared with those in the control group; however, this increase was attenuated in the Ang II + TQ group.

*TQ reduces fibrosis-related protein expression in the heart tissues of mice in the Ang II group*. To investigate the mechanism underlying fibrosis in heart damage, the expression levels of collagen I and III were examined using immunohistochemistry (Fig. 4A) and western blotting (Fig. 4B and C). The expression collagen I and III were increased in Ang II group compared with the control group. However, compared with in the Ang II group, mice in the Ang II + TQ group exhibited

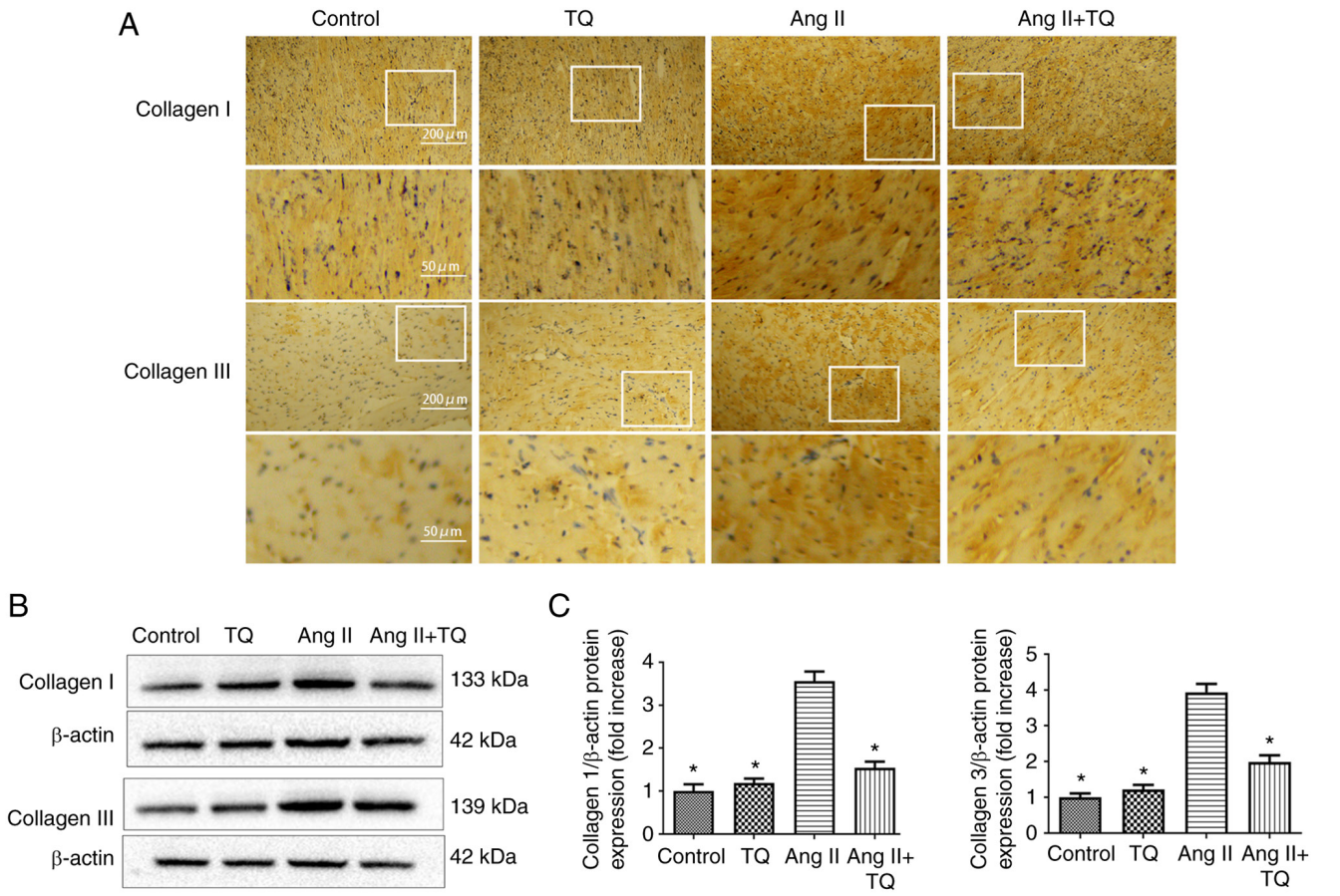


Figure 4. (A) Representative images of mouse heart tissues immunohistochemically stained for collagen I and III following different treatments. Magnification, x40. n=3/group. (B) Western blotting for collagen I and III in heart tissue. (C) Bar graph showing semi-quantification of the protein expression levels of collagen I and III. Data are presented as the mean ± SEM; n=3/group. *P<0.05 vs. the Ang II group. TQ, thymoquinone; Ang II, angiotensin II.

markedly reduced collagen I and III expression levels. These findings indicated that TQ reduced collagen I and III expression in Ang II-treated mice.

*TQ reduces Nox4 and p53 expression in the heart tissues of mice in the Ang II group*. Immunohistochemistry was used to analyze the protein expression levels of Nox4 and p53 (Fig. 5A). The expression Nox4 and p53 were increased in Ang II group compared with the control group. In the Ang II + TQ group this increase was markedly reduced in heart tissue compared with the Ang II group. A similar result was obtained by western blotting; the Ang II-induced increase in the expression levels of these proteins was attenuated by TQ treatment (Fig. 5B and C). These findings suggested that TQ may reduce metabolic energy-related protein expression in the heart tissue of Ang II-treated mice.

*Ang II upregulates the expression levels of pro-inflammatory cytokines in H9c2 cells*. RT-PCR was performed to evaluate the expression levels of pro-inflammatory cytokines in H9c2 cells exposed to different concentrations of Ang II. Cultured H9c2 cells were incubated with Ang II for 24 h. A dose-dependent upregulation of pro-inflammatory cytokine expression was observed with Ang II treatment (Fig. 6); the strongest upregulation was caused by Ang II at a concentration of 300 nmol/l.

*ERK expression in H9c2 cells*. The present study examined the involvement of the ERK pathway in H9c2 cells. ERK phosphorylation was revealed to be induced by treating H9c2 cells with 300 nmol/l Ang II. p-ERK levels in cells increased when 300 nmol/l of Ang II was used compared with treated with 0 nmol/l Ang II (Fig. 7A). Furthermore, pre-incubation with an ERK inhibitor (20 $\mu$M PD98059) for 30 min, followed by treatment with Ang II for 48 h, reduced ERK phosphorylation (Fig. 7B) compared with treatment without ERK inhibitor. These findings indicated that p-ERK expression levels were increased when H9c2 cells were incubated with 300 nmol/l Ang II, but were markedly decreased by PD98059 treatment.

*Fibrosis-related protein expression, and Nox4 and p53 expression in H9c2 cells*. The present study examined the expression levels of fibrosis-related proteins, and Nox4 and p53 in H9c2 cells (Fig. 8). The expression levels of collagen I and III, Nox4 and p53 were increased when H9c2 cells were incubated with 300 nmol/l Ang II, but were markedly decreased with PD98059 treatment.

*TQ reduces p-ERK expression in vivo and vitro*. The present study examined the expression levels of p-ERK in heart tissue and H9c2 cells (Fig. 9). p-ERK expression was clearly increased in Ang II group compared with the control group.

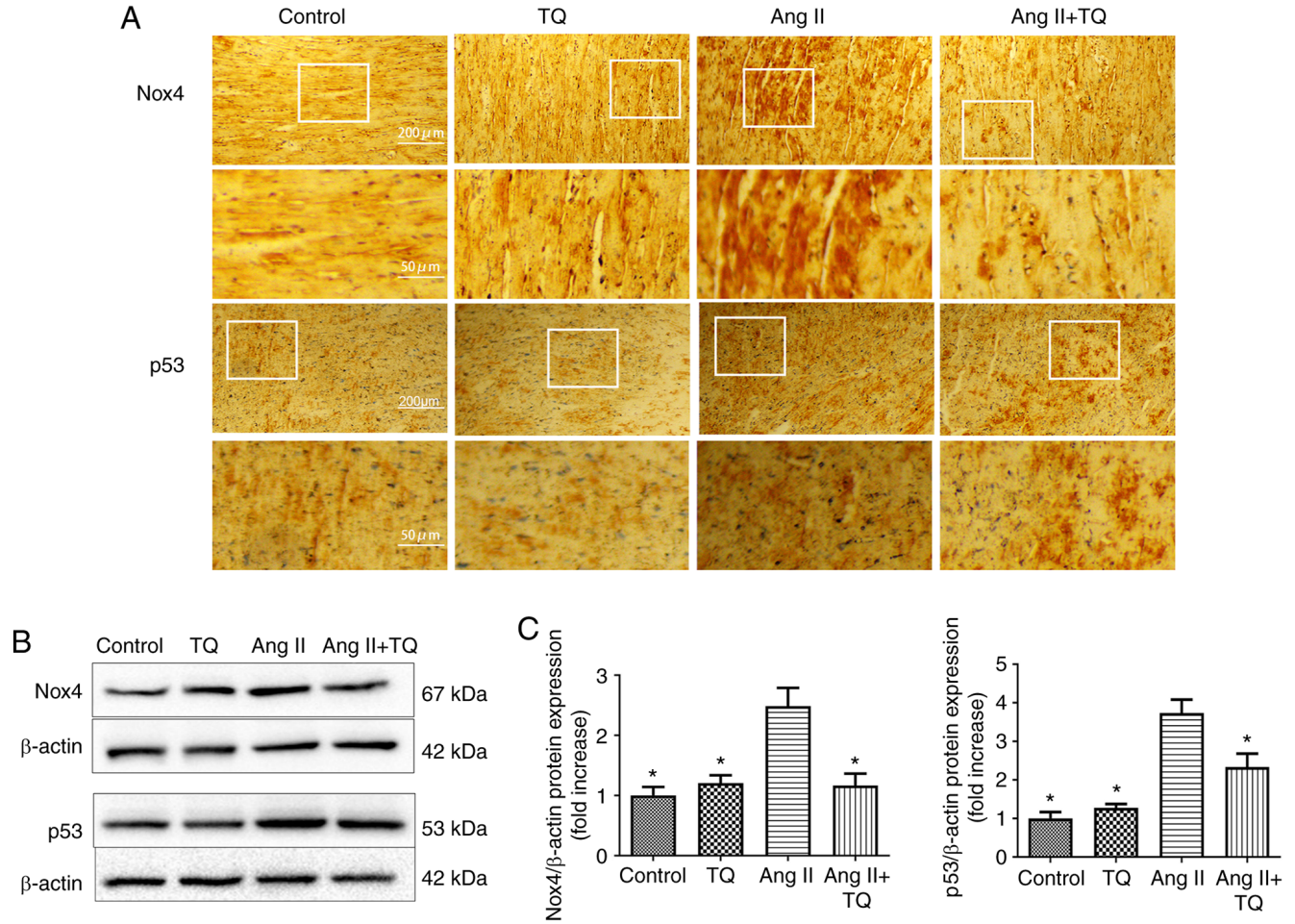


Figure 5. (A) Representative images of mouse heart tissues immunohistochemically stained for Nox4 and p53 following different treatments. Magnification, x40. n=3/group. (B) Western blotting for Nox4 and p53 in heart tissue. (C) Bar graph showing semi-quantification of the protein expression levels of Nox4 and p53. Data are presented as the mean ± SEM; n=3/group. *P<0.05 vs. the Ang II group. TQ, thymoquinone; Ang II, angiotensin II.

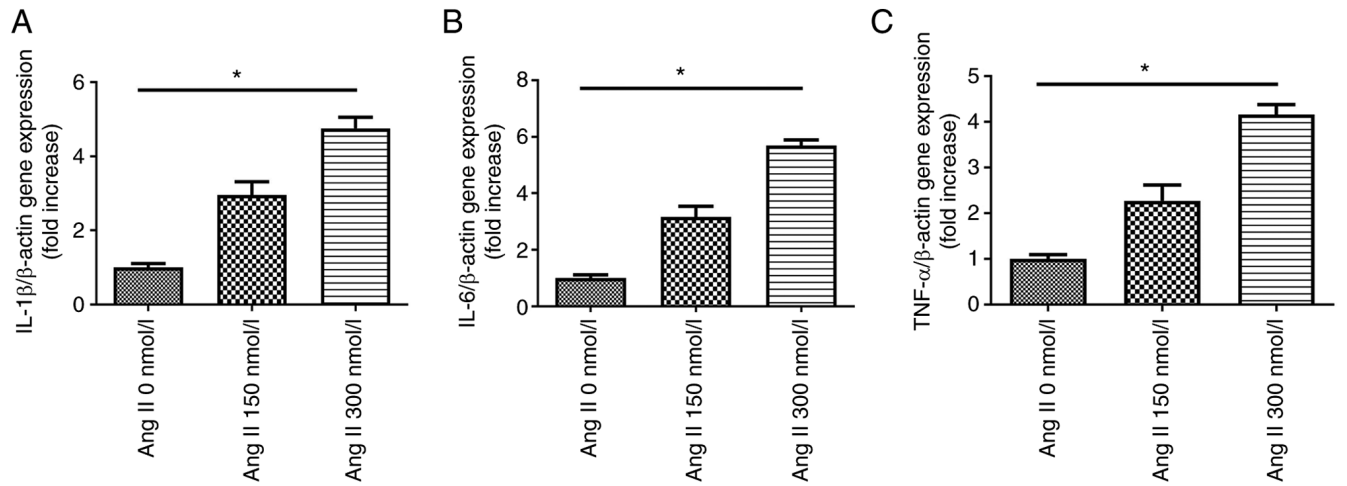


Figure 6. Relative mRNA expression levels of (A) IL-1β, (B) IL-6 and (C) TNF-α in H9c2 cells. H9c2 cells were incubated with Ang II (0, 150 and 300 nmol/l) for up to 24 h. Data are presented as the mean ± SEM; n=4-6/group. *P<0.05. TQ, thymoquinone; Ang II, angiotensin II; IL, interleukin; TNF-α, tumor necrosis factor α.

The Ang II + TQ group exhibited significantly reduced p-ERK expression in heart tissues compared with that in the Ang II group (Fig. 9A and B). The expression levels of p-ERK were increased when H9c2 cells were incubated with 300 nmol/l Ang II, but were decreased with TQ or PD98059 treatment respectively (Fig. 9C and D). Notably, p-ERK expression was markedly decreased by TQ and PD98059 treatment. TQ increased the inhibitory effect of the ERK inhibitor.

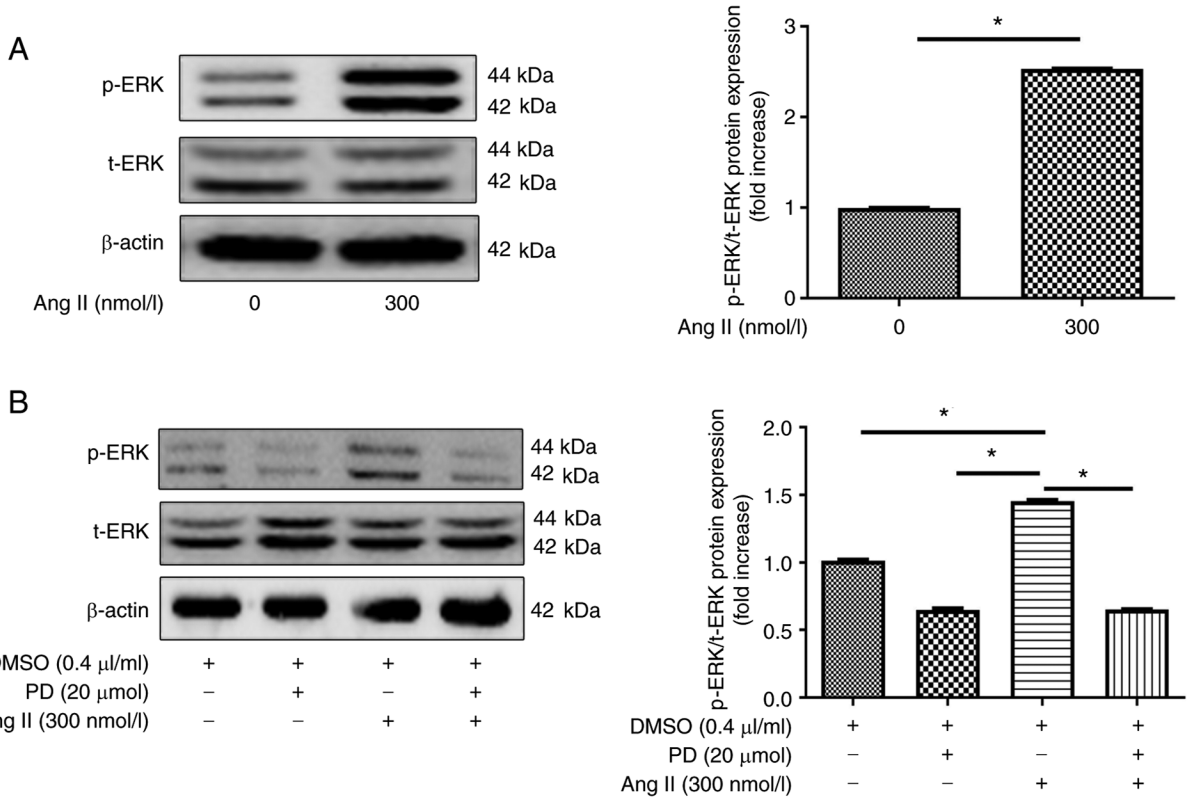


Figure 7. (A) Western blot analysis of p-ERK, t-ERK and β-actin. H9c2 cells were incubated with Ang II (0 or 300 nmol/l) for up to 48 h. The bar graph shows semi-quantification of p-ERK/t-ERK expression. (B) Western blot analysis of p-ERK following pre-treatment with an ERK inhibitor. H9c2 cells were grown in culture and pre-incubated with an ERK inhibitor (PD; 20 $\mu$mol/l) for 30 min followed by treatment with Ang II for 48 h. The bar graph shows semi-quantification of p-ERK/t-ERK expression. Data are presented as the mean ± SEM; n=3/group. *P<0.05. ERK, extracellular signal-regulated kinase; p, phosphorylated; PD, PD98059; t, total.

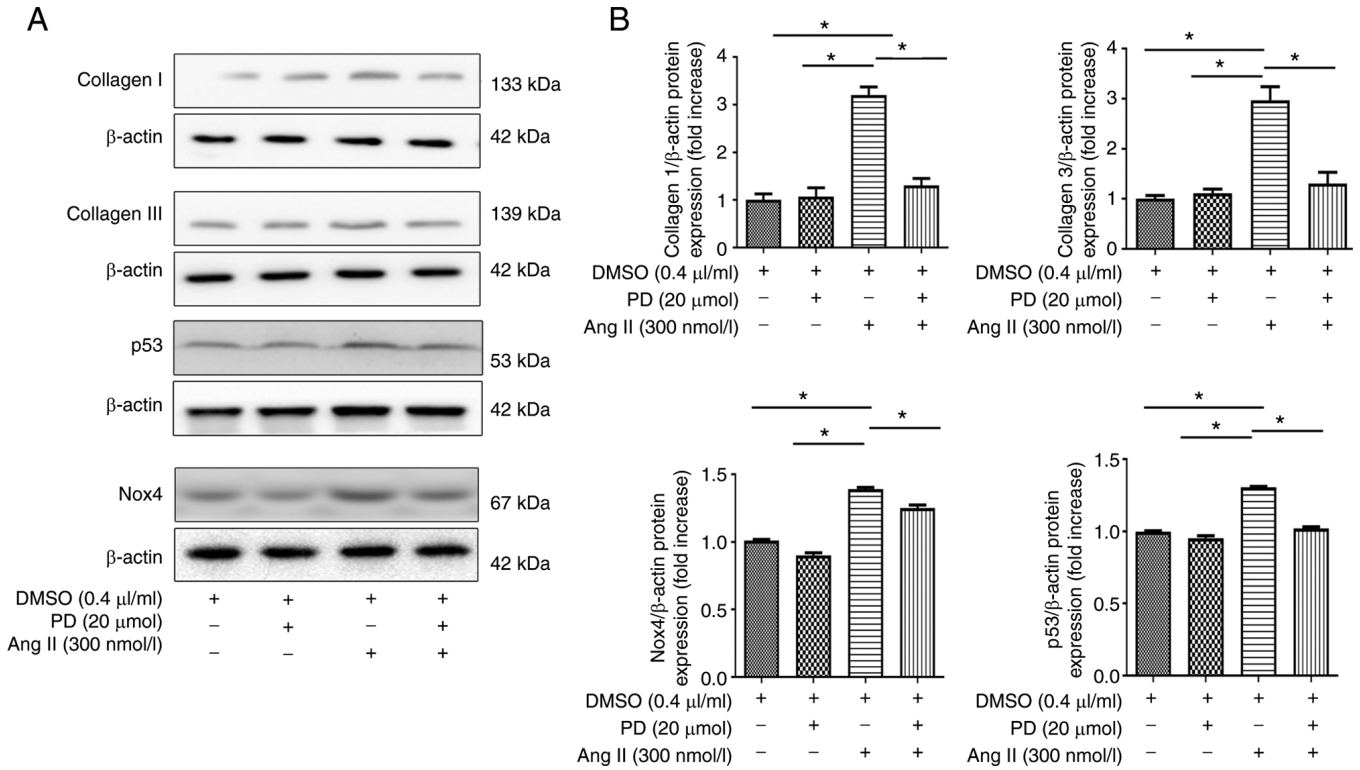


Figure 8. (A) Western blot analysis of collagen I and III, Nox4 and p53 in H9c2 cells incubated with Ang II (300 nmol/l) and ERK inhibitor. (B) Bar graph shows semi-quantification of the protein expression levels of collagen I and III, Nox4 and p53 in H9c2 cells. H9c2 cells were grown in culture and pre-incubated with an ERK inhibitor (PD98059; 20 $\mu$mol/l) for 30 min followed by treatment with Ang II for 48 h. Data are presented as the mean ± SEM; n=3/group. *P<0.05. ERK, extracellular signal-regulated kinase; p, phosphorylated; PD, PD98059; t, total.

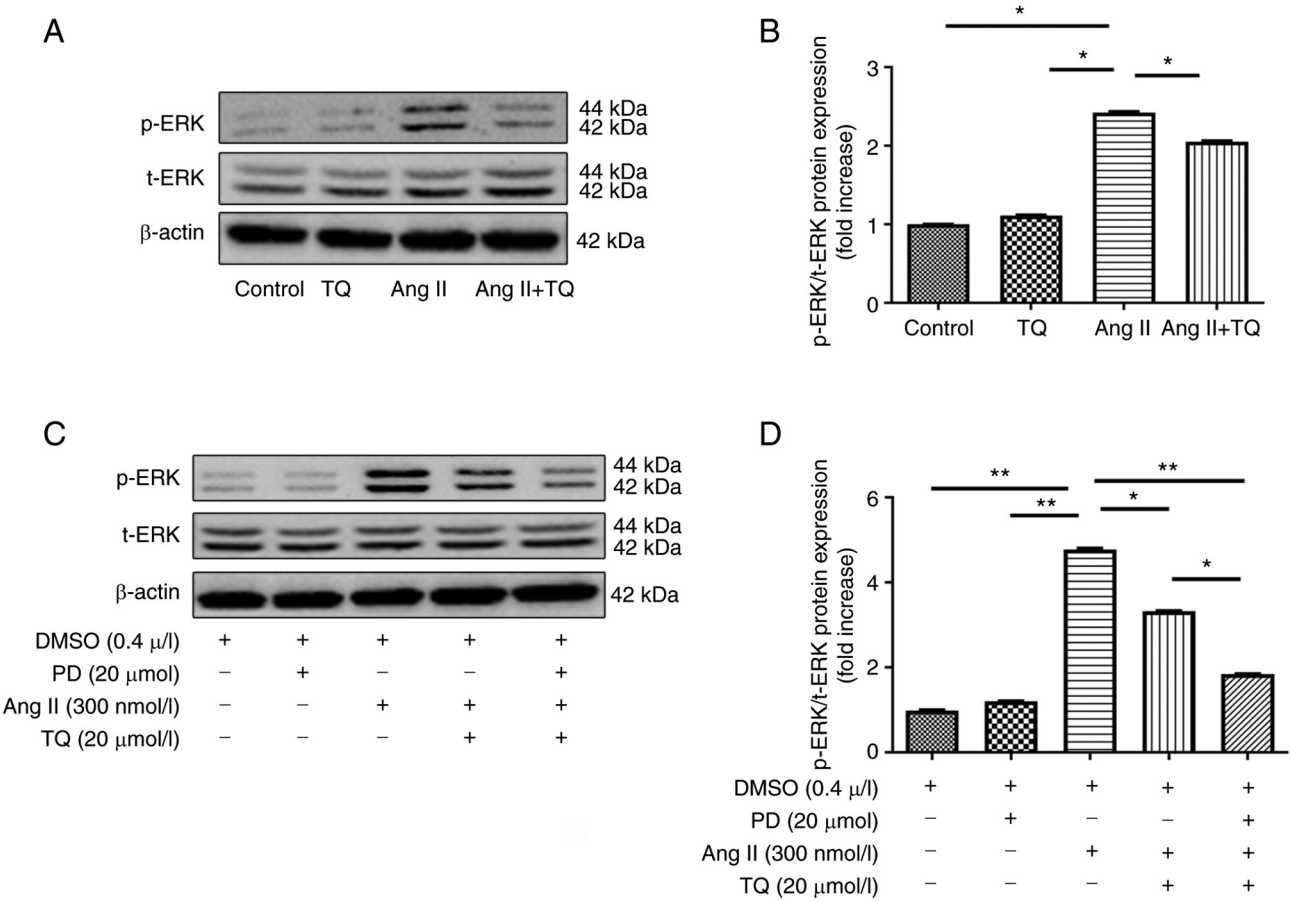


Figure 9. (A) Western blot analysis of p-ERK in heart tissue. (B) Bar graph shows the semi-quantification of the expression levels of p-ERK in heart tissue. (C) Western blot analysis of p-ERK following pre-treatment of cells with an ERK inhibitor and TQ. (D) Bar graph shows semi-quantification of the expression levels of collagen I and III, Nox4 and p53 in H9c2 cells. H9c2 cells were cultured and pre-incubated with an ERK inhibitor (PD; 20 $\mu$mol/l) for 30 min followed by treatment with Ang II for 48 h. For TQ treatment, cells were grown to 80% confluence and then incubated with TQ at the indicated concentration (20 $\mu$mol/l) for 24 h. For PD + Ang II + TQ group, the cells were pre-incubated with PD and then treatment with Ang II and TQ as previously mentioned. DMSO treatment (final concentration, 0.1%) was used as a sham control. Data are presented as the mean ± SEM; n=3/group. $^{*}$P<0.05, $^{**}$P<0.01. ERK, extracellular signal-regulated kinase; p, phosphorylated; PD, PD98059; t, total; TQ, thymoquinone.

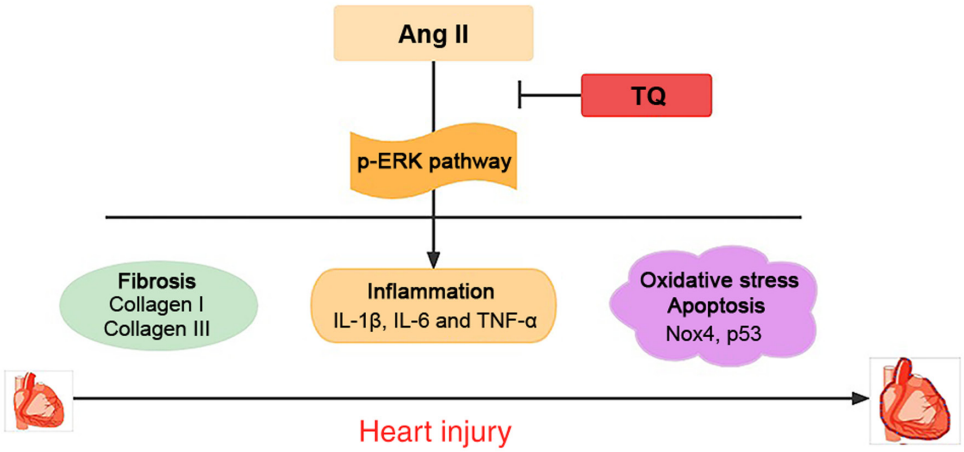


Figure 10. Schematic diagram demonstrating how TQ protects against cardiac damage induced by Ang II in apolipoprotein E-deficient mice. Ang II, angiotensin II; ERK, extracellular signal-regulated kinase; IL, interleukin; p, phosphorylated; TNF-α, tumor necrosis factor α; TQ, thymoquinone.

## Discussion

The present study demonstrated that TQ had a protective effect against cardiac damage via anti-inflammatory, anti-fibrotic, anti-oxidative stress and anti-apoptotic effects (as suggested by its effects on proteins associated with oxidative stress and apoptosis; Fig. 10). A cardiac damage model was established by implanting osmotic minipumps filled with

Ang II solutions in mice to investigate the effects of TQ. Body weight did not exhibit obvious changes in Ang II-infused mice, this may be because there was insufficient time to detect changes in body weight. In addition, the observation time has not been long enough in previous studies to show body weight changes (24,25). With regard to metabolic characteristics, the serum hs-CRP level has been used to indicate the instability of atherosclerotic lesions in several clinical studies and as a risk predictor of cardiovascular events (26-28). In the present study, the Ang II group exhibited significantly higher indices of cardiac injury (hs-CRP) compared with in the control group; however, treatment with TQ significantly reduced the hs-CRP levels, alleviating the cardiac damage induced by Ang II. Chobanian and Alexander (7) reported that Ang II may influence cardiovascular disease development by increasing arterial blood pressure, which is in agreement with the findings of the present study. Hypertension is a major cause of cardiac damage. Elevated blood pressure can cause cardiac fibrosis, which in turn leads to remodeling of the heart structure; uncontrolled cardiac remodeling can lead to heart failure (8,29). The present study observed an increase in blood pressure in the Ang II group compared with that in the control group, which was attenuated by TQ treatment. These findings suggested that TQ may attenuate cardiac fibrosis by suppressing the increase in blood pressure early, which was confirmed by histological analyses.

RAS serves a key role in the development of cardiovascular diseases. Ang II is a core effector of RAS and an increase in its concentration can cause inflammation (29). The mechanism underlying the pro-inflammatory effect of Ang II on cardiovascular diseases includes triggering of vascular damage and recruitment of inflammatory cells (8). In the present study, H&E staining revealed higher inflammatory cell infiltration in the Ang II group than in the control group. Notably, TQ reduced inflammatory cell infiltration in the Ang II + TQ group. Furthermore, it reduced the Ang II-induced increases in the expression levels of inflammatory molecules (IL-1β, IL-6 and TNF-α). Ojha *et al* (30) reported that TQ may exhibit cardioprotective effects by inhibiting the expression of pro-inflammatory cytokines (31).

Collagen I and III are derived from cardiac fibroblasts, and have an important role in cardiac function. Collectively, these extracellular matrix (ECM) proteins define the fibrous meshwork of the heart (31,32). The excess accumulation of ECM can cause cardiac fibrosis, thereby limiting cardiomyocyte contraction and relaxation (33,34). Ang II acts primarily by binding to its type I receptor, thus stimulating cardiac fibroblasts to produce ECM proteins and causing reactive fibrosis in the heart (35-37). In the present study, Masson staining was used to evaluate collagen deposition in the cardiac tissue following Ang II-induced cardiac damage. Masson staining revealed higher collagen deposition in the Ang II group than in the control group. Notably, TQ reduced collagen deposition in the Ang II + TQ group. In addition, immunohistochemistry and western blotting were used to examine the expression levels of collagen I and III. Compared with in the Ang II group mice, the Ang II + TQ group mice exhibited significantly reduced collagen I and III expression levels, indicating that TQ reduced fibrosis. This is consistent with our suggestion that TQ may attenuate cardiac fibrosis by suppressing the increase in blood pressure early.

Several studies have shown that oxidative stress is an important mechanism underlying cardiovascular disease development (38,39). Furthermore, inhibition of oxidative stress has been reported to alleviate the endothelial dysfunction caused by Ang II in mice (40). Nox4, which induces oxidative stress, has critical roles in the pathogenesis of cardiovascular diseases (38,41). Heymes *et al* (41) reported that Nox4 may have an important role in cardiomyocyte injury. In addition, Nox4 has been shown to mediate cardiac hypertrophy by inducing apoptosis (42). p53 is recognized as a key molecule in the adaptation to harmful stimuli, including oxidative stress, and has a pivotal role in myocardial apoptosis (43,44). In the present study, immunohistochemistry and western blotting were performed to analyze the expression levels of Nox4 and p53. The Ang II group exhibited significantly increased Nox4 and p53 expression in the heart tissue compared with that in the control group, which indicated that Ang II induced cardiac damage by increasing Nox4 and p53 levels; this is in agreement with the findings of Tian *et al* (45). TQ has been reported to attenuate cardiomyopathy in streptozotocin-treated diabetic rats via anti-oxidative stress (20). Similarly, the present study revealed that TQ reduced Nox4 and p53 expression in the heart tissue of Ang II-treated mice. Therefore, TQ may have a protective function against cardiac damage caused by Ang II via anti-oxidative stress and anti-apoptotic effects.

RAS is a central component of the physiological and pathological responses of the cardiovascular system. Ang II, as a primary effector hormone, serves a significant role in cardiac function (1,2). Its effect is achieved through complex intracellular signal transduction pathways. ERK is a member of the mitogen-activated protein kinase (MAPK) family and is closely related to cardiac damage (46,47). MAPKs are potential mediators of inflammatory responses and atherosclerosis (48,49). Furthermore, it has been reported that the ERK signaling pathway is related to liver fibrosis (50,51). In the present study, RT-qPCR was performed to evaluate the expression levels of pro-inflammatory cytokines in H9c2 cells exposed to Ang II at different concentrations. The results demonstrated that the inflammation caused by Ang II at a concentration of 300 nmol/l was the most severe. Activated MAP3K phosphorylates MEK 1/2 and catalyzes the phosphorylation of ERK1/2 at Tyr204/187 and then Thr202/185, and activated ERK1/2 (p-ERK) promotes the release of its downstream target genes (52). In the present study, the expression levels of p-ERK were increased when H9c2 cells were incubated with 300 nmol/l Ang II; however, treatment with an inhibitor of ERK (PD98059) decreased the levels of p-ERK. This revealed that Ang II-induced cardiac inflammation may be mediated via the p-ERK pathway, which increased the expression of pro-inflammatory cytokines. A previous study revealed that urantide can alleviate atherosclerotic myocardial injury by regulating the MAPK signaling pathway and inhibiting the expression of p-ERK (53). In addition, the present study detected the protein expression levels of Nox4, p53, collagen I and III when cells were stimulated with Ang II and an ERK inhibitor. The results revealed that the expression levels of these factors were inhibited by the ERK inhibitor, which suggested that Ang II could increase the expression of collagen I, collagen III, Nox4 and p53 by activating the ERK signaling pathway, thus causing cardiac damage. Previous

studies have reported that the p-ERK pathway is related to oxidative stress, inflammatory response and fibrosis (54-57), which is consistent with the present findings. Furthermore, it was revealed that TQ presented a synergistic action with the ERK inhibitor, whereby TQ increased the inhibitory effect of the ERK inhibitor. These findings indicated that TQ may act against Ang II-induced cardiac damage via the p-ERK signaling pathway.

Notably, there is a limitation of the present study; an ultrasonographic examination was not performed to determine if there were changes in cardiac hypertrophy. We plan to investigate this in future studies.

In conclusion, the present study established that TQ has a protective effect against Ang II-induced cardiac damage, as shown by the reduction in hs-CRP levels, and the inhibition of inflammatory cell infiltration, pro-inflammatory cytokine expression, fibrosis, oxidative stress and apoptosis associated proteins via suppressing activation of the p-ERK signaling pathway. These findings provide novel insights into cardiac damage caused by Ang II and present the possibility for a new therapeutic intervention for the treatment of cardiovascular diseases.

**Acknowledgements**

Not applicable.

**Funding**

The present study was supported by grants from the Xi'an Medical Science Research Program of China (grant no. XA2020-YXYJ-0413).

**Availability of data and materials**

The datasets used and/or analyzed during the present study are available from the corresponding author on reasonable request.

**Authors' contributions**

HD designed the study. LZ, ZP and YW provided their assistance in the execution of the experiments. LZ and YW confirmed the authenticity of all raw data. HZ and JM analyzed the data and interpreted the results. YW prepared the figures. LZ drafted the manuscript. All authors read and approved the final manuscript.

**Ethics approval and consent to participate**

All experimental procedures in this study were approved by the ethical committee of Xi'an No. 3 Hospital.

**Patient consent for publication**

Not applicable.

**Competing interests**

The authors declare that they have no competing interests.

**References**

1. Kim JA, Berliner JA and Nadler JL: Angiotensin II increases monocyte binding to endothelial cells. Biochem Biophys Res Commun 226: 862-868, 1996.
2. Lonn EM, Yusuf S, Jha P, Montague TJ, Teo KK, Benedict CR and Pitt B: Emerging role of angiotensin-converting enzyme inhibitors in cardiac and vascular protection. Circulation 90: 2056-2069, 1994.
3. Alderman MH, Madhavan S, Ooi WL, Cohen H, Sealey JE and Laragh JH: Association of the renin-sodium profile with the risk of myocardial infarction in patients with hypertension. N Engl J Med 324: 1098-1104, 1991.
4. Daugherty A, Manning MW and Cassis LA: Angiotensin II promotes atherosclerotic lesions and aneurysms in apolipoprotein E-deficient mice. J Clin Invest 105: 1605-162, 2000.
5. Cassis LA, Gupte M, Thayer S, Zhang X, Charnigo R, Howatt DA, Rateri DL and Daugherty A: ANG II infusion promotes abdominal aortic aneurysms independent of increased blood pressure in hypercholesterolemic mice. Am J Physiol Heart Circ Physiol 296: H1660-H1665, 2009.
6. Guan XH, Hong X, Zhao N, Liu XH, Xiao YF, Chen TT, Deng LB, Wang XL, Wang JB, Ji GJ, *et al*: CD38 promotes angiotensin II-induced cardiac hypertrophy. J Cell Mol Med 21: 1492-1502, 2017.
7. Chobanian AV and Alexander RW: Exacerbation of atherosclerosis by hypertension. Potential mechanisms and clinical implications. Arch Intern Med 156: 1952-1956, 1996.
8. Jia L, Li Y, Xiao C and Du J: Angiotensin II induces inflammation leading to cardiac remodeling. Front Biosci (Landmark Ed) 17: 221-231, 2012.
9. She G, Ren YJ, Wang Y, Hou MC, Wang HF, Gou W, Lai BC, Lei T, Du XJ and Deng XL: $K_{Ca}$3.1 channels promote cardiac fibrosis through mediating inflammation and differentiation of monocytes into myofibroblasts in angiotensin II-treated rats. J Am Heart Assoc 8: e010418, 2019.
10. Touyz RM, Anagnostopoulou A, Camargo LL, Rios FJ and Montezano AC: Vascular biology of superoxide-generating NADPH oxidase 5-implications in hypertension and cardiovascular disease. Antioxid Redox Signal 30: 1027-1040, 2019.
11. Gali-Muhtasib H, Roessner A and Schneider-Stock R: Thymoquinone: A promising anti-cancer drug from natural sources. Int J Biochem Cell Biol 38: 1249-1253, 2006.
12. el Tahir KE, Ashour MM and al-Harbi MM: The cardiovascular actions of the volatile oil of the black seed (*Nigella sativa*) in rats: Elucidation of the mechanism of action. Gen Pharmacol 24: 1123-1131, 1993.
13. Woo CC, Kumar AP, Sethi G and Tan KH: Thymoquinone: Potential cure for inflammatory disorders and cancer. Biochem Pharmacol 83: 443-451, 2012.
14. Hosseinzadeh H, Taiari S and Nassiri-Asl M: Effect of thymoquinone, a constituent of *Nigella sativa* L., on ischemia-reperfusion in rat skeletal muscle. Naunyn Schmiedebergs Arch Pharmacol 385: 503-508, 2012.
15. Xiao J, Ke ZP, Shi Y, Zeng Q and Cao Z: The cardioprotective effect of thymoquinone on ischemia-reperfusion injury in isolated rat heart via regulation of apoptosis and autophagy. J Cell Biochem 119: 7212-7217, 2018.
16. Adalı F, Gonul Y, Kocak A, Yuksel Y, Ozkececi G, Ozdemir C, Tunay K, Bozkurt MF and Sen OG: Effects of thymoquinone against cisplatin-induced cardiac injury in rats. Acta Cir Bras 31: 271-277, 2016.
17. Jalili C, Sohrabi M, Jalili F and Salahshoor MR: Assessment of thymoquinone effects on apoptotic and oxidative damage induced by morphine in mice heart. Cell Mol Biol (Noisy-le-grand) 64: 33-38, 2018.
18. Ortega R, Collado A, Selles F, Gonzalez-Navarro H, Sanz MJ, Real JT and Piqueras L: SGLT-2 (Sodium-Glucose Cotransporter 2) Inhibition reduces Ang II (Angiotensin II)-induced dissecting abdominal aortic aneurysm in ApoE (Apolipoprotein E) knockout mice. Arterioscler Thromb Vasc Biol 39: 1614-1628, 2019.
19. Stegbauer J, Thatcher SE, Yang G, Bottermann K, Rump LC, Daugherty A and Cassis LA: Mas receptor deficiency augments angiotensin II-induced atherosclerosis and aortic aneurysm ruptures in hypercholesterolemic male mice. J Vasc Surg 70: 1658-68.e1, 2019.
20. Atta MS, El-Far AH, Farrag FA, Abdel-Daim MM, Al Jaouni SK and Mousa SA: Thymoquinone attenuates cardiomyopathy in streptozotocin-treated diabetic rats. Oxid Med Cell Longev 2018: 7845681, 2018.

21. Satoh K, Nigro P, Zeidan A, Soe NN, Jaffré F, Oikawa M, O'Dell MR, Cui Z, Menon P, Lu Y, *et al*: Cyclophilin A promotes cardiac hypertrophy in apolipoprotein E-deficient mice. Arterioscler Thromb Vasc Biol 31: 1116-1123, 2011.
22. Koutnikova H, Laakso M, Lu L, Combe R, Paananen J, Kuulasmaa T, Kuusisto J, Häring HU, Hansen T, Pedersen O, *et al*: Identification of the UBP1 locus as a critical blood pressure determinant using a combination of mouse and human genetics. PLoS Genet 5: e1000591, 2009.
23. Livak KJ and Schmittgen TD: Analysis of relative gene expression data using real-time quantitative PCR and the 2(-Delta Delta C(T)) method. Methods 25: 402-408, 2001.
24. Chen P, Yang F, Wang W, Li X, Liu D, Zhang Y, Yin G, Lv F, Guo Z, Mehta JL and Wang X: Liraglutide attenuates myocardial fibrosis via inhibition of AT1R-mediated ROS production in hypertensive mice. J Cardiovasc Pharmacol Ther 26: 179-188, 2021.
25. Madeddu P, Emanueli C, Maestri R, Salis MB, Minasi A, Capogrossi MC and Olivetti G: Angiotensin II type 1 receptor blockade prevents cardiac remodeling in bradykinin B(2) receptor knockout mice. Hypertension 35: 391-396, 2000.
26. Ridker PM, Hennekens CH, Buring JE and Rifai N: C-reactive protein and other markers of inflammation in the prediction of cardiovascular disease in women. N Engl J Med 342: 836-843, 2000.
27. Matsushita K, Yatsuya H, Tamakoshi K, Yang PO, Otsuka R, Wada K, Mitsuhashi H, Hotta Y, Kondo T, Murohara T and Toyoshima H: High-sensitivity C-reactive protein is quite low in Japanese men at high coronary risk. Circ J 71: 820-825, 2007.
28. Shimada K, Fujita M, Tanaka A, Yoshida K, Jisso S, Tanaka H, Yoshikawa J, Kohro T, Hayashi D, Okada Y, *et al*: Elevated serum C-reactive protein levels predict cardiovascular events in the Japanese coronary artery disease (JCAD) study. Circ J 73: 78-85, 2009.
29. Touyz RM: Intracellular mechanisms involved in vascular remodelling of resistance arteries in hypertension: Role of angiotensin II. Exp Physiol 90: 449-455, 2005.
30. Ojha S, Azimullah S, Mohanraj R, Sharma C, Yasin J, Arya DS and Adem A: Thymoquinone protects against myocardial ischemic injury by mitigating oxidative stress and inflammation. Evid Based Complement Alternat Med 2015: 143629, 2015.
31. Ninh VK, El Hajj EC, Ronis MJ and Gardner JD: N-Acetylcysteine prevents the decreases in cardiac collagen I/III ratio and systolic function in neonatal mice with prenatal alcohol exposure. Toxicol Lett 315: 87-95, 2019.
32. Husse B, Briest W, Homagk L, Isenberg G and Gekle M: Cyclical mechanical stretch modulates expression of collagen I and III by PKC and tyrosine kinase in cardiac fibroblasts. Am J Physiol Regul Integr Comp Physiol 293: R1898-R1907, 2007.
33. Cowling RT, Kupsky D, Kahn AM, Daniels LB and Greenberg BH: Mechanisms of cardiac collagen deposition in experimental models and human disease. Transl Res 209: 138-155, 2019.
34. Wynn TA and Ramalingam TR: Mechanisms of fibrosis: Therapeutic translation for fibrotic disease. Nat Med 18: 1028-1040, 2012.
35. Villarreal FJ, Kim NN, Ungab GD, Printz MP and Dillmann WH: Identification of functional angiotensin II receptors on rat cardiac fibroblasts. Circulation 88: 2849-2861, 1993.
36. Schnee JM and Hsueh WA: Angiotensin II, adhesion, and cardiac fibrosis. Cardiovasc Res 46: 264-268, 2000.
37. Leask A: Getting to the heart of the matter: New insights into cardiac fibrosis. Circ Res 116: 1269-1276, 2015.
38. Brandes RP, Weissmann N and Schröder K: NADPH oxidases in cardiovascular disease. Free Radic Biol Med 49: 687-706, 2010.
39. Nabeebaccus A, Zhang M and Shah AM: NADPH oxidases and cardiac remodelling. Heart Fail Rev 16: 5-12, 2011.
40. Li DX, Chen W, Jiang YL, Ni JQ and Lu L: Antioxidant protein peroxiredoxin 6 suppresses the vascular inflammation, oxidative stress and endothelial dysfunction in angiotensin II-induced endotheliocyte. Gen Physiol Biophys 39: 545-555, 2020.
41. Heymes C, Bendall JK, Ratajczak P, Cave AC, Samuel JL, Hasenfuss G and Shah AM: Increased myocardial NADPH oxidase activity in human heart failure. J Am Coll Cardiol 41: 2164-2171, 2003.
42. Schröder K, Zhang M, Benkhoff S, Mieth A, Pliquett R, Kosowski J, Kruse C, Luedike P, Michaelis UR, Weissmann N, *et al*: Nox4 is a protective reactive oxygen species generating vascular NADPH oxidase. Circ Res 110: 1217-1225, 2012.
43. Farina F, Sancini G, Mantecca P, Gallinotti D, Camatini M and Palestini P: The acute toxic effects of particulate matter in mouse lung are related to size and season of collection. Toxicol Lett 202: 209-217, 2011.
44. Qin F, Patel R, Yan C and Liu W: NADPH oxidase is involved in angiotensin II-induced apoptosis in H9C2 cardiac muscle cells: Effects of apocynin. Free Radic Biol Med 40: 236-246, 2006.
45. Tian HP, Sun YH, He L, Yi YF, Gao X and Xu DL: Single-stranded DNA-binding protein 1 abrogates cardiac fibroblast proliferation and collagen expression induced by angiotensin II. Int Heart J 59: 1398-1408, 2018.
46. Purcell NH, Wilkins BJ, York A, Saba-El-Leil MK, Meloche S, Robbins J and Molkentin JD: Genetic inhibition of cardiac ERK1/2 promotes stress-induced apoptosis and heart failure but has no effect on hypertrophy in vivo. Proc Natl Acad Sci USA 104: 14074-14079, 2007.
47. Cipolletta E, Rusciano MR, Maione AS, Santulli G, Sorriento D, Del Giudice C, Ciccarelli M, Franco A, Crola C, Campiglia P, *et al*: Targeting the CaMKII/ERK interaction in the heart prevents cardiac hypertrophy. PLoS One 10: e0130477, 2015.
48. Jagavelu K, Tietge UJ, Gaestel M, Drexler H, Schieffer B and Bavendiek U: Systemic deficiency of the MAP kinase-activated protein kinase 2 reduces atherosclerosis in hypercholesterolemic mice. Circ Res 101: 1104-1112, 2007.
49. Matsuzawa A and Ichijo H: Molecular mechanisms of the decision between life and death: Regulation of apoptosis by apoptosis signal-regulating kinase 1. J Biochem 130: 1-8, 2001.
50. Wang Y, Song J, Bian H, Bo J, Lv S, Pan W and Lv X: Apelin promotes hepatic fibrosis through ERK signaling in LX-2 cells. Mol Cell Biochem 460: 205-215, 2019.
51. Ning ZW, Luo XY, Wang GZ, Li Y, Pan MX, Yang RQ, Ling XG, Huang S, Ma XX, Jin SY, *et al*: MicroRNA-21 mediates angiotensin II-induced liver fibrosis by activating NLRP3 inflammasome/IL-1β axis via targeting Smad7 and Spry1. Antioxid Redox Signal 27: 1-20, 2017.
52. Xu Z, Sun J, Tong Q, Lin Q, Qian L, Park Y and Zheng Y: The role of ERK1/2 in the development of diabetic cardiomyopathy. Int J Mol Sci 17: 2001, 2016.
53. Zhao J, Miao G, Wang T, Li J and Xie L: Urantide attenuates myocardial damage in atherosclerotic rats by regulating the MAPK signalling pathway. Life Sci 262: 118551, 2020.
54. Cheng M, Wu G, Song Y, Wang L, Tu L, Zhang L and Zhang C: Celastrol-induced suppression of the miR-21/ERK signalling pathway attenuates cardiac fibrosis and dysfunction. Cell Physiol Biochem 38: 1928-1938, 2016.
55. Li P, Chen XR, Xu F, Liu C, Li C, Liu H, Wang H, Sun W, Sheng YH and Kong XQ: Alamandine attenuates sepsis-associated cardiac dysfunction via inhibiting MAPKs signaling pathways. Life Sci 206: 106-116, 2018.
56. Liu M, Qin J, Hao Y, Liu M, Luo J, Luo T and Wei L: Astragalus polysaccharide suppresses skeletal muscle myostatin expression in diabetes: Involvement of ROS-ERK and NF-κB pathways. Oxid Med Cell Longev 2013: 782497, 2013.
57. Rao RK and Clayton LW: Regulation of protein phosphatase 2A by hydrogen peroxide and glutathionylation. Biochem Biophys Res Commun 293: 610-616, 2002.